Title

Skeletal myofiber VEGF is necessary for myogenic and contractile adaptations to functional overload of the plantaris in adult mice

Journal

Journal of Applied Physiology, 120(2)

ISSN

8750-7587

Authors

Huey, Kimberly A
Smith, Sophia A
Sulaeman, Alexis
et al.

Publication Date

2016-01-15

DOI

10.1152/japplphysiol.00638.2015

Peer reviewed

J Appl Physiol 120: 188–195, 2016.
First published November 5, 2015; doi:10.1152/japplphysiol.00638.2015.

Skeletal myofiber VEGF is necessary for myogenic and contractile adaptations to functional overload of the plantaris in adult mice

Kimberly A. Huey,[1] Sophia A. Smith,[1] Alexis Sulaeman,[2] and Ellen C. Breen[2]

[1]*College of Pharmacy and Health Sciences, Drake University, Des Moines, Iowa; and* [2]*Department of Medicine, University of California-San Diego, La Jolla, California*

Submitted 27 July 2015; accepted in final form 21 October 2015

Huey KA, Smith SA, Sulaeman A, Breen EC. Skeletal myofiber VEGF is necessary for myogenic and contractile adaptations to functional overload of the plantaris in adult mice. *J Appl Physiol* 120: 188–195, 2016. First published November 5, 2015; doi:10.1152/japplphysiol.00638.2015.—The ability to enhance muscle size and function is important for overall health. In this study, skeletal myofiber vascular endothelial growth factor (VEGF) was hypothesized to regulate hypertrophy, capillarity, and contractile function in response to functional overload (FO). Adult myofiber-specific VEGF gene-ablated mice (skmVEGF$^{-/-}$) and wild-type (WT) littermates underwent plantaris FO or sham surgery (SHAM). Mass, morphology, in vivo function, IGF-1, basic fibroblast growth factor (bFGF), hepatocyte growth factor (HGF), and Akt were measured at 7, 14, and 30 days. FO resulted in hypertrophy in both genotypes, but fiber sizes were 13% and 23% smaller after 14 and 30 days, respectively, and mass 15% less after 30 days in skmVEGF$^{-/-}$ than WT. FO increased isometric force after 30 days in WT and decreased in skmVEGF$^{-/-}$ after 7 and 14 days. FO also resulted in a reduction in specific force and this differed between genotypes at 14 days. Fatigue resistance improved only in 14-day WT mice. Capillary density was decreased by FO in both genotypes. However, capillary-to-fiber ratios were 19% and 15% lower in skmVEGF$^{-/-}$ than WT at the 14- and 30-day time points, respectively. IGF-1 was increased by FO at all time points and was 45% and 40% greater in skmVEGF$^{-/-}$ than WT after 7 and 14 days, respectively. bFGF, HGF, total Akt, and phospho-Akt, independent of VEGF expression, and VEGF levels in WT were increased after 7 days of FO. These findings suggest VEGF-dependent capillary maintenance supports muscle growth and function in overloaded muscle and is not rescued by compensatory IGF-1 expression.

functional overload; plantaris; VEGF; muscle force

SKELETAL MUSCLE normally responds to chronic elevations in load by increasing mass, strength, and/or fatigue resistance (46). However, inadequate responses can lead to muscle dysfunction and weakness, resulting in a muscle that cannot meet the demands necessary for normal mobility. Loading-induced impairment in muscle function can occur with aging or as a result of several chronic diseases characterized by muscle wasting or cachexia (6, 26, 41). Under these conditions smaller and weaker muscles often do not have the capacity to perform normal locomotor activities. Hypertrophy induced by functional overload (FO) of the plantaris provides an in vivo model to elucidate the molecular mechanisms by which an increase in muscle mass and improved function occur in response to increased contractile demands in healthy muscle or is compromised in models of disease.

While it is well known that vascular endothelial growth factor (VEGF) is an essential angiogenic factor for skeletal muscle development (22), it also plays a role in maintaining capillaries in adult skeletal muscle (51), and is important for the angiogenic response to endurance training (16). However, the role of skeletal myofiber VEGF in the time-dependent sequence of cellular events that occur during FO-induced hypertrophy has not been elucidated. Our laboratory and others have reported that plantaris or soleus VEGF mRNA and protein levels increase in response to overload before an increase in muscle mass (14, 40). In the extensor digitorum longus (EDL), a more glycolytic muscle phenotype than the plantaris, studies of FO in the presence of a VEGF receptor decoy (VEGF-Trap) or in mice deficient in myofiber (both cardiac and skeletal) VEGF has been suggested to contribute to the formation of new capillaries that occurs with chronic muscle use (25, 55). However, in a healthy muscle, growth occurs through coordination of several stages involving myogenesis, activation and differentiation of satellite cells (53), and angiogenesis, the formation of new capillaries, is thought to be required to supply O_2 and nutrients to hypertrophied fibers (15, 19, 42).

Within the first week following FO, inflammation (7), macrophage infiltration (39, 52), possible damage/injury (33, 50), increased levels of IGF-1 (3, 4, 39), and activation of the Akt-mammalian target of rapamycin (mTOR) signaling pathway have been reported (2, 4, 5, 9, 39, 48). During this initial stage, the gain in muscle weight is generally indicative of inflammation (7) rather than augmented muscle protein levels (4). After 2 wk of FO, muscle mass is significantly increased and continues to increase for up to 30 days (3, 48). Interestingly, several studies have shown that early responses to hypertrophic stimuli have important implications for longer-term adaptations (21, 48). For example, in satellite cell-depleted mouse plantaris, normal fiber hypertrophy was observed after the first 2 wk of overload (34), but subsequent long-term adaptations were impaired (21). Thus the time course of the current study allows elucidation of the potential time-dependent role of VEGF in the cellular and contractile muscle adaptations to a hypertrophic stimulus.

In this present study, we hypothesized that adult skeletal myofiber VEGF is a critical mediator of muscle capillarity and myofiber size that governs FO-induced increases in muscle mass, force production, and fatigue resistance. Furthermore, the expression of additional growth factors, insulin like growth factor (IGF), basic fibroblast growth factor (bFGF), and hepatocyte growth factor (HGF), as well as total and phospho-Akt, that could potentially partially or fully compensate for the loss of skeletal myofiber VEGF in the response to FO were measured. To test these hypotheses the VEGF gene was conditionally deleted in adult skeletal myofibers and synergistic muscles were removed to impose abrupt and dramatic increases in load

Address for reprint requests and other correspondence: K. A. Huey, College of Pharmacy and Health Sciences, Drake Univ., 2507 Univ. Ave., Des Moines, IA 50311 (e-mail: kimberly.huey@drake.edu).

on the plantaris. Mice were assessed for changes in plantaris muscle mass and fiber size, capillary number, in vivo contractile function, and growth factor levels at 7, 14, and/or 30 days. A key feature of this mouse model is that mice were allowed to develop a normal vascular system before specifically targeting VEGF deletion in skeletal myofibers.

METHODS

Animals. All procedures were approved by the Drake University Institutional Animal Care and Use Committee and the University of California-San Diego Institutional Animal Care and Use Committee and followed the American Physiological Society Animal Care Guidelines.

Adult male VEGF gene-ablated mice (skmVEGF$^{-/-}$) or wild-type littermates (WT), 4 mo of age, were divided into four groups based on genotype and surgical intervention: *1*) WT-Sham surgery, *2*) WT FO surgery, *3*) skmVEGF$^{-/-}$-Sham surgery, and *4*) skmVEGF$^{-/-}$ FO surgery. At each experimental time point (7, 14, or 30 days) mice in each of the 4 experimental groups were studied. In the WT and skmVEGF$^{-/-}$ sham groups at the 7, 14, and 30-day time points statistical analysis found no differences among any variable (n = 5-6 at each time point). Thus, in an effort to minimize unnecessary animal use, the data from the 7, 14, and 30-day time points were pooled into a single sham group for each genotype resulting in 16–18 animals per sham group. The WT and skmVEGF$^{-/-}$ FO groups included 8–12 animals per genotype at each experimental time point.

Generation of inducible, skeletal myofiber-specific VEGF gene ablation mice. Homozygous VEGF*LoxP* mice (22) were crossed with a heterozygous HSA-Cre-ER^{T2} mouse line (47) in which Cre-ER^{T2} is selectively expressed in skeletal myonuclei (controlled by human skeletal muscle α-actin sequence) and *Cre* recombinase activity is tamoxifen dependent. The WT mice have a floxed VEGF gene on both alleles and are homozygous for the VEGF*LoxP* transgene. Tamoxifen (1 mg, ip) was administered to both skmVEGF$^{-/-}$ and WT male mice for five consecutive days (*day 0* through *day 4*) and mice were subjected to functional overload beginning on *day 21*.

Genotyping. The presence or absence of the HSA-Cre-ER^{T2} transgene in each mouse was determined by PCR analysis using tail DNA and forward 5′-CTAGAGCCTGTTTTGCACGTTC-3′ and reverse 5′-TGCAAGTTGAATAACCGGAAA-3′ primers under the following conditions: one 2-min polymerase activation incubation at 95°C, 35 cycles of 30 s denaturation at 94°C, 30 s annealing at 52.1°C, 60 s elongation at 72°C, followed by one 8-min elongation period at 72°C as previously described (16, 47).

Sham or FO surgery. To mechanically overload the plantaris, mice underwent bilateral ablation of the soleus and gastrocnemius as previously described (27). Briefly, animals were anesthetized with isoflurane and under aseptic conditions an incision was made in the lower leg to expose the ankle extensors (soleus, plantaris, and gastrocnemius). The soleus and one-third of the lower medial and lateral gastrocnemius were removed while preserving vascular and neural supplies to the plantaris. The incision site was closed with subcuticular sutures, and the mice were allowed to recover in individual cages. Sham surgery included the incision and placement of sutures without removing the muscles.

Force and fatigue measurements. Plantaris isometric force production was measured in the left leg only as previously described by our laboratory (36). Briefly, mice were anesthetized with isoflurane (Vet Med Equip System, Livermore, CA), and the sciatic nerve was exposed through the popliteal fossa to electrically stimulate the nerve and elicit contraction of the plantaris. In the FO groups, plantarflexor force was due to plantaris contraction as the gastrocnemius and soleus had been removed during FO surgery. In the sham groups, the gastrocnemius and soleus tendons were cut prior to the testing procedure to measure only plantaris muscle force. The hindfoot was placed on a footplate attached to a servomotor that was able to measure applied torque and control ankle rotation (300C-LR, Aurora Scientific, Aurora, ON). The sciatic nerve was carefully placed on a stimulating dual hook electrode (Grass Technologies part no. F-ES-48, Warwick, RI), connected to a square-wave stimulator (A-M Systems, Sequim, WA), and stimulated at 200 Hz for 1.5 s with a pulse duration of 0.5 ms to evoke a maximum-force contraction. The nerve was kept moist with mineral oil warmed to ~37°C. The servomotor was set to maintain position, ensuring that the contraction was isometric. A total of 10 contractions were completed with 5-s delays between stimulations. Muscle fatigue was evaluated by comparing the 10th contraction to the initial maximum contraction and expressing this difference as a percent of the maximal force. For all animals, the maximal force generation occurred during the first contraction. Force was normalized to both body mass and plantaris weight.

Tissue collection. Immediately after the force measurements, the mice were euthanized by cervical dislocation and the plantaris and quadriceps muscles from both legs were quickly isolated and immediately frozen on dry ice and stored at −80°C until analysis. Muscles from the leg that underwent muscle testing were used for ELISA analysis and the contralateral leg muscles were used for immunohistochemistry. Based on previous experience in our laboratory, acute muscle testing elicits negligible effects on steady-state protein levels in the muscles (37). Since the contractions performed during muscle testing could potentially impact morphometry (e.g., minor fiber damage) only the untested contralateral limb muscles were used for immunohistochemistry.

Skeletal muscle immunohistochemistry. Plantaris were prepared for immunohistochemistry by mounting on a cork with OCT freezing medium and cryo-preserving in liquid nitrogen-cooled isopentane. The muscle was positioned vertically with the support of a kidney cut in half and placed cut side down on the OCT-coated cork. The portion of the muscle that was sectioned was not coated in OCT. Ten-micrometer sections were collected from the mid-portion of the plantaris. Capillaries and fibers were detected using the capillary lead-ATPase method (44). Images were captured at a 20× magnification using a Hamamatsu Nanozoomer Slide Scanning System. ImageJ was used for the morphometric analysis of the entire plantaris cross-section and measurements of capillary and fiber number, capillary density, fiber size, and total muscle area were collected and used to calculate the capillary density and capillary-to-fiber ratio. The entire plantaris muscle cross section included analysis of ~700 to 900 fibers.

ELISA analysis. Mouse VEGF, IGF-1, HGF, and bFGF concentrations were measured in skeletal muscle lysates using validated kits (RayBiotech, Norcross, GA). The relative levels of total and phosphorylated Akt were measured in skeletal muscle lysates using validated kits (RayBiotech). The plantaris was used for all ELISAs with the exception of the VEGF ELISA. In this case the quadriceps was used to confirm the loss of myofiber VEGF in skmVEGF$^{-/-}$ mice (Fig. 1). Plantaris or quadriceps muscle samples (~10 mg) were mechanically homogenized in a standard RIPA buffer containing 50 mM Tris-HCl (pH 7.8) and supplemented with a protease and phosphatase inhibitor cocktail (Sigma, St. Louis, MO). Homogenates were immediately centrifuged at 12,000 *g* at 4°C for 12 min, and the supernatant, the detergent soluble fraction, was removed. Protein concentrations were determined by Bradford assay (Pierce, Grand Island, NY) using a bovine serum albumin (BSA) standard curve and immediately stored at −20°C for subsequent use in ELISA assays. Growth factors levels are expressed as picograms per milligram total protein. According to manufacturer's directions, a positive control dilution series was performed for the Akt ELISA, and data are presented as blanked OD values at 450 nm.

Statistical analyses. Measurements were collected in four experimental groups (Sham or FO in WT and skmVEGF$^{-/-}$ mice) on *days 7, 14*, or *30* after sham or FO surgery. Measurements included: *1*) maximal isometric muscle force, *2*) muscle fatigability, *3*) VEGF,

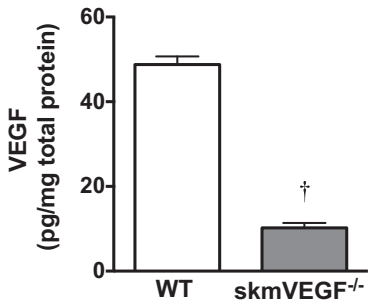

Fig. 1. Skeletal muscle VEGF levels are decreased in myofiber VEGF gene-deleted mice (skmVEGF$^{-/-}$). VEGF levels measured by ELISA were decreased by 80% in quadriceps from skmVEGF$^{-/-}$ mice compared with wild-type (WT) littermates. Values are means ± SE; $n = 28$ for WT and $n = 22$ for skmVEGF$^{-/-}$. †Significant difference between genotypes ($P < 0.05$).

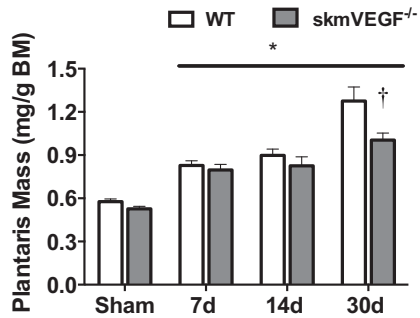

Fig. 2. Changes in plantaris muscle mass after 7, 14, or 30 days of functional overload (FO) in WT and skmVEGF$^{-/-}$ mice. Average plantaris mass normalized to body mass (BM) for sham and FO mice. Values are means ± SE; $n = 8$–12/FO group at each time point and 16–18 in sham groups. *Significant effect of FO (significantly different from sham within genotype). †Significant difference between genotypes ($P < 0.05$).

IGF-1, HGF, and bFGF protein concentrations, *4*) total and phosphorylated Akt levels, *5*) capillary-to-fiber ratio and capillary density, *6*) muscle fiber area, and *7*) muscle mass. Each of two surgical interventions (sham or FO) and 2 genotypes (WT or skmVEGF$^{-/-}$) were statistically analyzed with a 2×2 factorial arrangement of treatments in a randomized complete block design. This permitted statistical evaluation of the main effects of surgery (sham vs. FO) and genotype and their interaction. Two-way ANOVA were performed to assess main effects and interactions. Significantly different main effects were further analyzed using the Bonferroni post hoc test to determine the source of the difference. All analyses were performed with GraphPad Prism 6.0 (San Diego, CA) with the significance level set at $P < 0.05$.

RESULTS

Conditional ablation of the VEGF gene in adult skeletal myofibers. To determine the effectiveness of the conditional ablation of the VEGF gene in skeletal muscle, VEGF protein levels were measured in the quadriceps, a muscle not involved in the experimental procedures. VEGF levels were significantly lower in the quadriceps muscle of skmVEGF$^{-/-}$ mice than WT mice with respective levels of 10.2 ± 1.1 and 48.8 ± 1.9 pg/mg total protein (Fig. 1).

Changes in body mass, plantaris mass, and plantaris mean fiber area. Average initial and final body weights for sham and FO groups in both genotypes were not different among groups (Table 1). There were significant main effects of FO and genotype on absolute plantaris mass and plantaris mass normalized to body mass (Table 1 and Fig. 2). SkmVEGF$^{-/-}$ plantaris weighed 15% less than the WT plantaris after 30 days of FO. Absolute and normalized plantaris masses were not different between genotypes after 7 or 14 days of FO. On all days, absolute and normalized plantaris masses in FO groups were greater than sham for both genotypes.

In vivo muscle force and fatigue. There were significant main effects of FO and genotype and a significant interaction of FO and genotype on both absolute and normalized to body mass maximal isometric force (Fig. 3*A*). Absolute maximal isometric forces for WT mice were 1.67 ± 0.14, 1.71 ± 0.10, 1.92 ± 0.19, and 2.41 ± 0.13 N·mm for sham, 7 day FO, 14 day FO, and 30 day FO groups, respectively. Absolute maximal isometric forces for skmVEGF$^{-/-}$ mice were 2.0 ± 0.16, 1.35 ± 0.17, 1.38 ± 0.18, and 2.00 ± 0.16 N·mm for sham, 7 day FO, 14 day FO, and 30 day FO groups, respectively. After 30 days of FO, absolute and normalized to body mass forces in WT mice were significantly greater than sham. In skmVEGF$^{-/-}$ mice, absolute and normalized to body mass isometric forces were significantly lower than sham after 7 or 14 days of FO. After 30 days of FO absolute and normalized to body mass isometric forces were greater than 7 day or 14 day values, but were not different from sham. After 14 and 30 days of FO, absolute and normalized to body mass isometric forces were significantly lower in skmVEGF$^{-/-}$ mice compared with WT mice.

There were significant main effects of FO and genotype on maximal isometric force normalized to plantaris mass (Fig. 3*B*). There was no significant interaction. At all time points, FO was associated with significantly lower maximal isometric force normalized to plantaris mass in both genotypes. After 14 days of FO, maximal isometric force normalized to plantaris mass was significantly lower in skmVEGF$^{-/-}$ mice compared with WT mice.

There were significant main effects of FO and genotype on muscle fatigability (Fig. 3*C*). FO was associated with significantly lower muscle fatigability than sham after 14 days in WT mice only.

Table 1. *Initial and final body masses and final plantaris masses*

	WT				skmVEGF$^{-/-}$			
	Sham	7 day FO	14 day FO	30 day FO	Sham	7 day FO	14 day FO	30 day FO
Initial BM, g	22.1 ± 0.4	22.4 ± 0.3	21.8 ± 0.7	21.3 ± 0.6	22.4 ± 0.4	22.2 ± 0.5	22.1 ± 0.6	21.3 ± 0.7
Final BM, g	21.6 ± 0.5	22.4 ± 0.3	22.1 ± 0.6	21.8 ± 0.5	22.6 ± 0.4	21.9 ± 0.4	22.5 ± 0.6	22.5 ± 0.6
Plantaris mass, mg	12.1 ± 0.4	18.8 ± 0.7*	19.6 ± 0.8*	27.3 ± 0.9*†	11.9 ± 0.5	17.1 ± 0.7*	17.7 ± 1.0*	23.3 ± 0.7*†

Values are means ± SE; $n = 8$–12 per functional overload (FO) group at each time point (7, 14, or 30 days) and 16–18 in sham groups. BM, body mass; WT, wild type; skmVEGF$^{-/-}$, VEGF gene-ablated mice. *Significant effect of FO (significantly different from sham). †Significant difference between genotypes ($P < 0.05$).

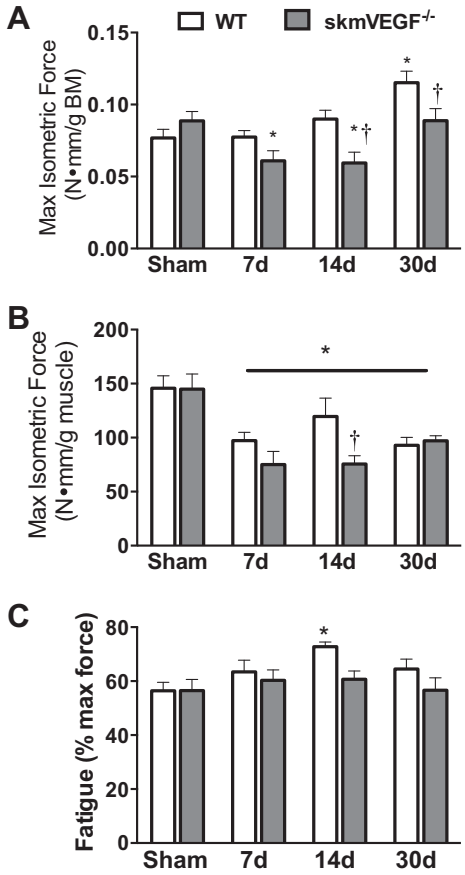

Fig. 3. Changes in plantaris maximal isometric force and fatigue resistance after 7, 14, or 30 days of functional overload (FO) in WT and skmVEGF$^{-/-}$ mice. Average maximal isometric force in N·mm relative to body mass (BM) (*A*) or plantaris mass (*B*) and fatigue calculated as % maximal force after 10th repetition (*C*) in sham and FO mice. Values are means ± SE; n = 8–12/FO group at each time point and 16–18 in sham groups. *Significant effect of FO (significantly different from sham within genotype). †Significant difference between genotypes ($P < 0.05$).

Capillary regression in response to functional overload. Representative sections from WT and skmVEGF$^{-/-}$ muscle after 30 days of FO are shown in Fig. 4*A*. There were significant main effects of FO and genotype and a significant interaction of FO and genotype on the capillary-to-fiber ratio in the plantaris (Fig. 4*B*). In skmVEGF$^{-/-}$ plantaris, the capillary-to-fiber ratio after 14 or 30 days of FO was significantly lower than the sham group. The capillary to fiber ratio was 19% and 15% lower in skmVEGF$^{-/-}$ than WT plantaris after 14 and 30 days of FO, respectively.

Measurements of plantaris mean fiber areas revealed significant main effects of FO and genotype and an interaction between these two variables (Fig. 4*C*). Fiber area was significantly increased in response to 14 or 30 days of FO in WT and skmVEGF$^{-/-}$ plantaris compared with sham. After 14 or 30 days of FO mean fiber areas were 13% and 23% lower, respectively, in skmVEGF$^{-/-}$ than WT plantaris.

There was a significant effect of FO on capillary density in the plantaris (Fig. 4*D*). In both genotypes, capillary density in the plantaris was significantly lower than sham groups after 14 or 30 days of FO.

Growth factor and (p)Akt levels in functionally overloaded plantaris. VEGF protein levels were significantly lower in the plantaris of skmVEGF$^{-/-}$ mice compared with WT mice under all conditions and did not change with FO (Fig. 5). In WT mice 7 days of FO was associated with a 33% increase in VEGF protein in the plantaris before returning to control (sham) levels at 14 days (Fig. 5).

There were significant main effects of FO and genotype and a significant interaction of FO and genotype on plantaris IGF-1 levels (Fig. 6*A*). After 7, 14, or 30 days of FO, IGF-1 levels were significantly higher than sham in both genotypes. After 7 or 14 days of FO, IGF-1 levels were 45 and 40% higher, respectively, in skmVEGF$^{-/-}$ than WT mouse plantaris. After 30 days of FO, IGF-1 levels were similar between genotypes.

There were significant main effects of FO on bFGF and HGF protein levels in the plantaris muscle (Fig. 6, *B* and *C*). FO-associated increases in both bFGF and HGF levels after 7 days of FO were independent of genotype. In both genotypes bFGF and HGF levels returned to baseline after 14 days of FO. The levels of bFGF and HGF were not measured at 30 days since levels had returned to baseline by 14 days.

There were significant main effects of FO on total and phosphorylated Akt protein in the plantaris muscle (Fig. 7, *A* and *B*). FO-associated increases in both muscle total and phosphorylated Akt levels after 7 days of FO were independent of genotype. In both genotypes after 14 days of FO, total Akt levels returned to baseline and phosphorylated Akt decreased below baseline. The levels of total and phosphorylated Akt were not measured at 30 days since levels returned to or below baseline by 14 days. There was a significant effect of FO on the ratio of phosphorylated to total Akt (Fig. 7*C*). FO-associated decreases in phosphorylated/total Akt below baseline after 14 days were independent of genotype.

DISCUSSION

These novel findings suggest a critical role for VEGF in the maintenance of capillaries that support muscle growth and improved contractile function in hypertrophying adult mouse fast locomotor muscle. Conditional deletion of skeletal myofiber VEGF in adult mice was associated with attenuated increases in plantaris mass and mean fiber area despite compensatory increases in IGF-1. While functional overload did not induce an angiogenic response in WT mice, the capillary-to-fiber ratio fell significantly below sham levels in overloaded skmVEGF$^{-/-}$ muscle. The blunted hypertrophic response coupled with a lack of capillary maintenance in skmVEGF$^{-/-}$ plantaris likely contributed to compromised functional adaptations. This is evident by the reduced muscle force response to FO in skeletal myofiber VEGF-deficient mice.

Contribution of VEGF to capillary maintenance and improved contractile function in response to overload. Maintenance of capillary-to-fiber ratio with FO was associated with significant increases in maximal isometric force relative to body mass in WT mice. In contrast, the significant fall in capillary-to-fiber ratio in skmVEGF$^{-/-}$ mice was associated with force loss at 7 and 14 days before recovering only back to sham levels at 30 days of FO. Capillary density fell below sham levels in both genotypes, but in WT mice this was due to fiber hypertrophy while in skmVEGF$^{-/-}$ mice it was due to a loss of capillaries and fiber hypertrophy that was significantly

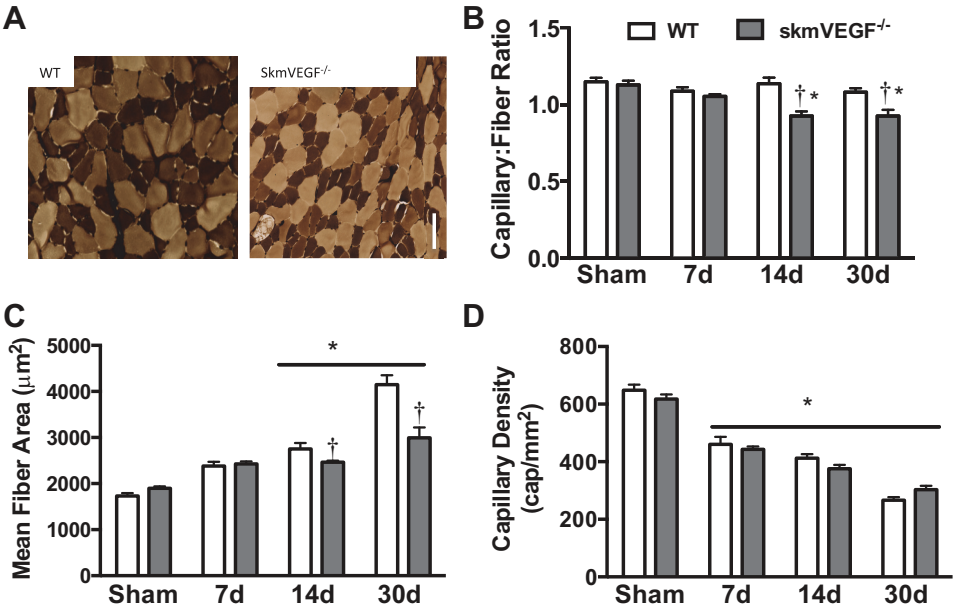

Fig. 4. Changes in capillary-to-fiber ratio, mean fiber area, and capillary density after 7, 14, or 30 days of functional overload (FO) in WT and skmVEGF$^{-/-}$ mice. Representative muscle sections after 30 days of FO in WT and skmVEGF$^{-/-}$ mice with loss of capillaries detected by capillary lead ATPase staining method; bar equals 25 μm (*A*). Average capillary-to-fiber ratio (*B*), mean fiber area (*C*), and capillary density (*D*) for sham and FO mice. Values are means ± SE; n = 8–12/FO group at each time point and n = 9 in sham groups. *Significant effect of FO (significantly different from sham within genotype). †Significant difference between genotypes ($P < 0.05$).

lower than WT responses. The capillary rarefication observed in the present study could contribute to the attenuated muscle growth (muscle mass and fiber size), which in turn likely impaired maximal muscle force production. The attenuated growth may reflect reductions in oxygen and nutrient delivery to the overloaded skmVEGF$^{-/-}$ muscle due to capillary loss. Interestingly, while isometric force normalized to body mass was significantly lower in skmVEGF$^{-/-}$ than WT at all time points, force normalized to muscle mass was only lower at 14 days. After 30 days of FO when the impaired muscle growth in skmVEGF$^{-/-}$ compared with WT was significant, the smaller muscle fibers in the skmVEGF$^{-/-}$ mice may have had more adequate delivery of oxygen and nutrients relative to fiber size. While maintenance of capillary density was not critical for FO-stimulated increases in force production, as evident by WT responses, when reduced capillary density was coupled with a loss of VEGF in skmVEGF$^{-/-}$ muscle, other factors may play a more significant role in contractile function. In WT mice, muscle fatigue resistance significantly increased after 14 days of FO with no change in skmVEGF$^{-/-}$ mice at any time point further suggesting potential impairment in oxygen and nutrient delivery to the muscle. It is unclear why fatigue resistance did not remain elevated in the WT mice after 30 days of FO. In summary, while angiogenesis may not match muscle growth during rapid hypertrophy even with VEGF, the loss of VEGF places the muscle in an even more compromised position functionally due to the loss of capillaries coupled with a reduced fiber area.

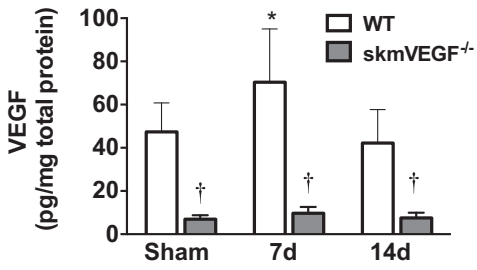

Fig. 5. Skeletal muscle VEGF levels after 7 or 14 days of functional overload (FO) in WT mice. Average VEGF levels for sham and FO mice. Values are means ± SE; n = 8–12/FO group at each time point and n = 16 in sham groups. *Significant effect of FO (significantly different from sham within genotype). †Significant difference between genotypes ($P < 0.05$).

Contribution of VEGF to myogenic adaptations to overload. In this study a time course was selected that reflects different cellular and contractile adaptations known to occur in response to a hypertrophic stimulus. The 7-day time point reflects early adaptations to overload which includes an inflammatory response that subsides by 14 days (7). This early response is also likely to include some degree of muscle damage/injury as the force requirements of the muscle exceed normal demands and myogenic adaptations have yet to fully occur (27, 28, 35, 39, 52). Several studies suggest the initiation and resolution of inflammation and repair process are important for subsequent muscle growth (10, 39). VEGF involvement in the early response to overload is suggested by the increases in VEGF protein in WT muscle and previous reports of upregulation of VEGF expression in functionally overloaded muscle (14, 40). The current experiments, as well as previous studies, have shown that increases in skeletal muscle VEGF are not always temporally associated with angiogenesis (14, 32) and suggest possible nonangiogenic roles of VEGF in muscle growth. For instance VEGF was first described by Dvorak and colleagues (18) as a permeability factor and could aid in resolving the initial weight gain thought to be due to inflammation/edema. Furthermore, exogenous delivery of VEGF to regenerating muscle has been shown to significantly promote repair and recovery (8). In vitro evidence suggests that VEGF signaling is necessary for myogenesis and increased myotube size in C2C12 muscle cells (12). Our group and others have demonstrated that FO is associated with activation of satellite cells (29, 30, 54), and the potential importance of satellite-endothelial cell interactions in cooperative angiomyogenesis (13, 43) suggests fewer activated satellite cells may subsequently reduce the formation of new capillaries. Satellite cells reside in a vascular niche in close association with the capillary endothe-

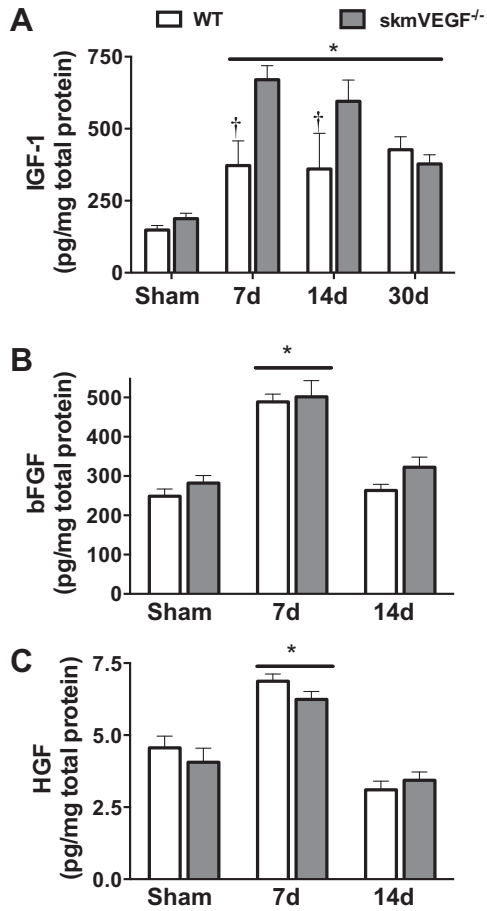

Fig. 6. Skeletal muscle IGF-1, bFGF, and HGF levels after 7, 14, or 30 days of functional overload (FO) in WT and skmVEGF$^{-/-}$ mice. Average IGF-1 (*A*), basic fibroblast growth factor (bFGF; *B*), or hepatocyte growth factor (HGF; *C*) levels for sham and FO mice. Values are means ± SE; $n = 8$–12/FO group at each time point and $n = 16$ in sham groups. *Significant effect of FO (i.e., significantly different from sham within genotype). †Significant difference between genotypes ($P < 0.05$).

lial cell, and differentiating myogenic cells may stimulate angiogenesis (13). Taken together, the loss of both satellite cells and capillaries could likely impair both muscle growth and the formation of new capillaries in a hypertrophying muscle.

Potential for angiogenic adaptation in different models of muscle overload. Almost all of the studies to date investigating angiogenesis in response to functional muscle overload utilized a model in which the EDL is overloaded by synergist ablation (11, 25, 55). In contrast to functional overload of the plantaris, which was done in this present study, overload of the EDL induces angiogenesis, but has not been shown to stimulate a robust hypertrophic response (19, 20). In many ways this model of chronic use of the EDL is more similar to endurance type training and elicits VEGF-dependent increases in skeletal muscle capillaries (11, 16, 25, 55). Only a single study found increases in the capillary-to-fiber ratio in the rat plantaris with functional overload alone (42), and another study reported no increases in capillary proliferation after 2 wk of synergist ablation in rat plantaris (14). In addition, 8 wk of resistance training in humans was associated with significant increases in quadriceps muscle cross-sectional area without any increase in capillary-to-fiber ratio (32). The absence of an angiogenic response in our mouse plantaris FO model is not unexpected, and the variable angiogenic responses to hypertrophic stimulus may be related to numerous factors including but not limited to the degree of hypertrophy and/or relative changes in muscle utilization. EDL mass has been reported to increase 14–31% with up to 30 days of overload while nearly all studies utilizing overload of the rodent plantaris report a more than doubling of muscle mass with at least 14 days of overload. Further, relative changes in muscle utilization with overload may also play a role as Egginton and colleagues reported that angiogenesis is a graded response to increases in muscle activation during overload (19, 20). In rodents the anti-gravity ankle extensors (e.g., plantaris, gastrocnemius, soleus) are routinely utilized more than flexors (e.g., tibialis anterior, EDL) (31, 45). Therefore, the relative changes in loading and activation with overload would likely be greater in the EDL and provide a greater stimulus for angiogenesis.

IGF-1 compensation during the early and mid-stages of the hypertrophic response. The FO model is widely used to increase loading and activation in rodent hindlimb muscles and results in increases in muscle cross-sectional area and force production. Importantly, this model has also been shown to

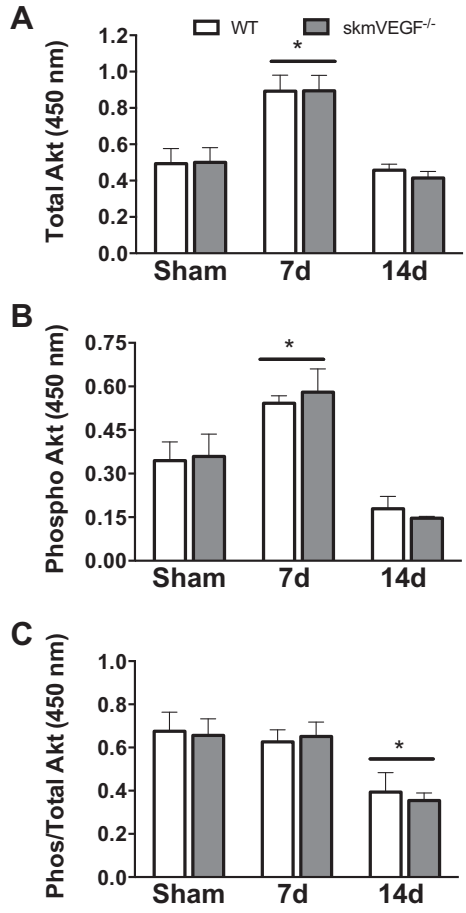

Fig. 7. Skeletal muscle (p)Akt levels after 7 or 14 days of functional overload (FO) in WT and skmVEGF$^{-/-}$ mice. Average relative levels of total Akt (*A*), phosphorylated Akt (*B*), and (p)Akt/total Akt (*C*) levels for sham and FO mice. Values are means ± SE; $n = 8$–12/FO group at each time point and $n = 16$ in sham groups. *Significant effect of FO (significantly different from sham within genotype) ($P < 0.05$).

activate anabolic molecules and pathways implicated in increased protein synthesis and muscle growth (49). Consequently, we measured muscle levels of several important growth factors in the plantaris to determine if the loss of VEGF was associated with compensatory increases in other growth factors. While FGF and HGF significantly increased in both genotypes after 7 days of FO before returning to baseline at 14 days, only IGF-1 showed compensatory increases in skmVEGF$^{-/-}$ muscles. Among these growth factors, there is much evidence that IGF-1 is important for significant muscle hypertrophy (1, 23). Specifically, FO has been shown to stimulate autocrine production of IGF-1 (3, 17, 24) and increase the activation of the Akt-mTOR signaling pathway (2, 4, 9, 38, 39, 48), with associated increases in muscle protein and DNA content (3). While this augmented IGF-1 response in skmVEGF$^{-/-}$ mice could potentially contribute to maintaining muscle mass (which was not different from the WT group in the skmVEGF$^{-/-}$ mice until the 30 day time point), the likely mechanism did not involve Akt as evidenced by similar increases in Akt expression and phosphorylation in both genotypes. This is in agreement with previous work showing that increased IGF-1 levels and IGF-1 signaling (Akt, mTOR, p70S6K, and/or 4EBP1) following irradiation to block satellite cell proliferation (2) or Cox-2 inhibition (39) did not protect against an impaired hypertrophic response. Importantly, the enhanced IGF-1 response did not protect against a loss in contractile function in VEGF-deficient muscle.

Summary. In summary, these experiments provide novel evidence that the conditional loss of VEGF in adult muscle fibers is associated with impaired myogenic and contractile adaptations to a significant hypertrophic stimulus both in the early and late phase of the compensatory growth response. Augmented expression of the muscle growth factor, IGF-1, was associated with the maintenance of muscle and fiber size during the early phases of the hypertrophic response but this did not persist at the latest time point. Furthermore, muscle force production, a key functional adaptation to overload, showed significant impairment at all time points in VEGF-deficient plantaris.

ACKNOWLEDGMENTS

We thank Dr. N. Ferrara for providing breeding pairs of the VEGF*LoxP* mice and Drs. P. Chambon and D. Metzeger for providing the HSA-Cre-ER^{T2} mice. We thank E. Stucker and D. Tuttle for animal care.

GRANTS

This work was supported by National Institute of Arthritis and Musculoskeletal and Skin Diseases Grant R15-AR-060469 to K. Huey.

DISCLOSURES

No conflicts of interest, financial or otherwise, are declared by the author(s).

AUTHOR CONTRIBUTIONS

Author contributions: K.A.H. and E.C.B. conception and design of research; K.A.H., S.A.S., A.S., and E.C.B. performed experiments; K.A.H. and S.A.S. analyzed data; K.A.H. interpreted results of experiments; K.A.H. prepared figures; K.A.H. drafted manuscript; K.A.H. and E.C.B. edited and revised manuscript; K.A.H., A.S., and E.C.B. approved final version of manuscript.

REFERENCES

1. **Adams GR.** Autocrine/paracrine IGF-I and skeletal muscle adaptation. *J Appl Physiol (1985)* 93: 1159–1167, 2002.
2. **Adams GR, Caiozzo VJ, Haddad F, Baldwin KM.** Cellular and molecular responses to increased skeletal muscle loading after irradiation. *Am J Physiol Cell Physiol* 283: C1182–C1195, 2002.
3. **Adams GR, Haddad F.** The relationships among IGF-1, DNA content, and protein accumulation during skeletal muscle hypertrophy. *J Appl Physiol* 81: 2509–2516, 1996.
4. **Adams GR, Haddad F, Baldwin KM.** Time course of changes in markers of myogenesis in overloaded rat skeletal muscles. *J Appl Physiol* 87: 1705–1712, 1999.
5. **Adams GR, Haddad F, Bodell PW, Tran PD, Baldwin KM.** Combined isometric, concentric, and eccentric resistance exercise prevents unloading-induced muscle atrophy in rats. *J Appl Physiol* 103: 1644–1654, 2007.
6. **Ali S, Garcia JM.** Sarcopenia, cachexia and aging: diagnosis, mechanisms and therapeutic options: a mini-review. *Gerontology* 60: 294–305, 2014.
7. **Armstrong RB, Marum P, Tullson P, Saubert CWt.** Acute hypertrophic response of skeletal muscle to removal of synergists. *J Appl Physiol* 46: 835–842, 1979.
8. **Arsic N, Zacchigna S, Zentilin L, Ramirez-Correa G, Pattarini L, Salvi A, Sinagra G, Giacca M.** Vascular endothelial growth factor stimulates skeletal muscle regeneration in vivo. *Mol Ther* 10: 844–854, 2004.
9. **Bodine SC, Stitt TN, Gonzalez M, Kline WO, Stover GL, Bauerlein R, Zlotchenko E, Scrimgeour A, Lawrence JC, Glass DJ, Yancopoulos GD.** Akt/mTOR pathway is a crucial regulator of skeletal muscle hypertrophy and can prevent muscle atrophy in vivo. *Nat Cell Biol* 3: 1014–1019, 2001.
10. **Bondesen BA, Mills ST, Kegley KM, Pavlath GK.** The COX-2 pathway is essential during early stages of skeletal muscle regeneration. *Am J Physiol Cell Physiol* 287: C475–C483, 2004.
11. **Brown MD, Hudlicka O.** Modulation of physiological angiogenesis in skeletal muscle by mechanical forces: involvement of VEGF and metalloproteinases. *Angiogenesis* 6: 1–14, 2003.
12. **Bryan BA, Walshe TE, Mitchell DC, Havumaki JS, Saint-Geniez M, Maharaj AS, Maldonado AE, D'Amore PA.** Coordinated vascular endothelial growth factor expression and signaling during skeletal myogenic differentiation. *Mol Biol Cell* 19: 994–1006, 2008.
13. **Christov C, Chretien F, Abou-Khalil R, Bassez G, Vallet G, Authier FJ, Bassaglia Y, Shinin V, Tajbakhsh S, Chazaud B, Gherardi RK.** Muscle satellite cells and endothelial cells: close neighbors and privileged partners. *Mol Biol Cell* 18: 1397–1409, 2007.
14. **Degens H, Moore JA, Alway SE.** Vascular endothelial growth factor, capillarization, and function of the rat plantaris muscle at the onset of hypertrophy. *Jpn J Physiol* 53: 181–191, 2003.
15. **Degens H, Turek Z, Hoofd LJ, Van't Hof MA, Binkhorst RA.** The relationship between capillarisation and fibre types during compensatory hypertrophy of the plantaris muscle in the rat. *J Anat* 180: 455–463, 1992.
16. **Delavar H, Nogueira L, Wagner PD, Hogan MC, Metzger D, Breen EC.** Skeletal myofiber VEGF is essential for the exercise training response in adult mice. *Am J Physiol Regul Integr Comp Physiol* 306: R586–R595, 2014.
17. **DeVol DL, Rotwein P, Sadow JL, Novakofski J, Bechtel PJ.** Activation of insulin-like growth factor gene expression during work- induced skeletal muscle growth. *Am J Physiol Endocrinol Metab* 259: E89–E95, 1990.
18. **Dvorak HF, Sioussat TM, Brown LF, Berse B, Nagy JA, Sotrel A, Manseau EJ, Van de Water L, Senger DR.** Distribution of vascular permeability factor (vascular endothelial growth factor) in tumors: concentration in tumor blood vessels. *J Exp Med* 174: 1275–1278, 1991.
19. **Egginton S, Badr I, Williams J, Hauton D, Baan GC, Jaspers RT.** Physiological angiogenesis is a graded, not threshold, response. *J Physiol* 589: 195–206, 2011.
20. **Egginton S, Hudlicka O, Brown MD, Walter H, Weiss JB, Bate A.** Capillary growth in relation to blood flow and performance in overloaded rat skeletal muscle. *J Appl Physiol (1985)* 85: 2025–2032, 1998.
21. **Fry CS, Lee JD, Jackson JR, Kirby TJ, Stasko SA, Liu H, Dupont-Versteegden EE, McCarthy JJ, Peterson CA.** Regulation of the muscle fiber microenvironment by activated satellite cells during hypertrophy. *FASEB J* 28: 1654–1665, 2014.
22. **Gerber HP, Hillan KJ, Ryan AM, Kowalski J, Keller GA, Rangell L, Wright BD, Radtke F, Aguet M, Ferrara N.** VEGF is required for growth and survival in neonatal mice. *Development* 126: 1149–1159, 1999.
23. **Glass DJ.** Signalling pathways that mediate skeletal muscle hypertrophy and atrophy. *Nat Cell Biol* 5: 87–90, 2003.

24. **Goldberg AL.** Work-induced growth of skeletal muscle in normal and hypophysectomized rats. *Am J Physiol* 213: 1193–1198, 1967.
25. **Gorman JL, Liu ST, Slopack D, Shariati K, Hasanee A, Olenich S, Olfert IM, Haas TL.** Angiotensin II evokes angiogenic signals within skeletal muscle through co-ordinated effects on skeletal myocytes and endothelial cells. *PLoS One* 9: e85537, 2014.
26. **He WA, Berardi E, Cardillo VM, Acharyya S, Aulino P, Thomas-Ahner J, Wang J, Bloomston M, Muscarella P, Nau P, Shah N, Butchbach ME, Ladner K, Adamo S, Rudnicki MA, Keller C, Coletti D, Montanaro F, Guttridge DC.** NF-kappaB-mediated Pax7 dysregulation in the muscle microenvironment promotes cancer cachexia. *J Clin Invest* 123: 4821–4835, 2013.
27. **Huey KA, Burdette S, Zhong H, Roy RR.** Early response of heat shock proteins to functional overload of the soleus and plantaris in rats and mice. *Exp Physiol* 95: 1145–1155, 2010.
28. **Huey KA, McCall GE, Zhong H, Roy RR.** Modulation of HSP25 and TNF-α during the early stages of functional overload of a rat slow and fast muscle. *J Appl Physiol* 102: 2307–2314, 2007.
29. **Hyatt JP, McCall GE, Kander EM, Zhong H, Roy RR, Huey KA.** PAX3/7 expression coincides with myod during chronic skeletal muscle overload. *Muscle Nerve* 38: 861–866, 2008.
30. **Ishido M, Uda M, Kasuga N, Masuhara M.** The expression patterns of Pax7 in satellite cells during overload-induced rat adult skeletal muscle hypertrophy. *Acta Physiol (Oxf)* 195: 459–469, 2009.
31. **Jasmin BJ, Gardiner PF.** Patterns of EMG activity of rat plantaris muscle during swimming and other locomotor activities. *J Appl Physiol* 63: 713–718, 1987.
32. **Kon M, Ohiwa N, Honda A, Matsubayashi T, Ikeda T, Akimoto T, Suzuki Y, Hirano Y, Russell AP.** Effects of systemic hypoxia on human muscular adaptations to resistance exercise training. *Physiol Rep* 2: e12033, 2014.
33. **Lowe DA, Alway SE.** Animal models for inducing muscle hypertrophy: are they relevant for clinical applications in humans? *J Orthop Sports Phys Ther* 32: 36–43, 2002.
34. **McCarthy JJ, Mula J, Miyazaki M, Erfani R, Garrison K, Farooqui AB, Srikuea R, Lawson BA, Grimes B, Keller C, Van Zant G, Campbell KS, Esser KA, Dupont-Versteegden EE, Peterson CA.** Effective fiber hypertrophy in satellite cell-depleted skeletal muscle. *Development* 138: 3657–3666, 2011.
35. **McCully KK, Faulkner JA.** Characteristics of lengthening contractions associated with injury to skeletal muscle fibers. *J Appl Physiol (1985)* 61: 293–299, 1986.
36. **Meador BM, Huey KA.** Glutamine preserves skeletal muscle force during an inflammatory insult. *Muscle Nerve* 40: 1000–1007, 2009.
37. **Meador BM, Huey KA.** Statin-associated changes in skeletal muscle function and stress response after novel or accustomed exercise. *Muscle Nerve* 44: 882–889, 2011.
38. **Miyazaki M, McCarthy JJ, Fedele MJ, Esser KA.** Early activation of mTORC1 signalling in response to mechanical overload is independent of phosphoinositide 3-kinase/Akt signalling. *J Physiol* 589: 1831–1846, 2011.
39. **Novak ML, Billich W, Smith SM, Sukhija KB, McLoughlin TJ, Hornberger TA, Koh TJ.** COX-2 inhibitor reduces skeletal muscle hypertrophy in mice. *Am J Physiol Regul Integr Comp Physiol* 296: R1132–R1139, 2009.
40. **Parvaresh K, Huber A, Brochin R, Bacon P, McCall G, Huey K, Hyatt JP.** Acute VEGF expression during hypertrophy is muscle phenotype-specific and localizes as a striated pattern within fibres. *Exp Physiol* 95: 1098–1106, 2010.
41. **Pellegrinelli V, Rouault C, Rodriguez-Cuenca S, Albert V, Edom-Vovard F, Vidal-Puig A, Clement K, Butler-Browne G, Lacasa D.** Human adipocytes induce inflammation and atrophy in muscle cells during obesity. *Diabetes* 64: 3121–3134, 2015.
42. **Plyley MJ, Olmstead BJ, Noble EG.** Time course of changes in capillarization in hypertrophied rat plantaris muscle. *J Appl Physiol (1985)* 84: 902–907, 1998.
43. **Rhoads RP, Johnson RM, Rathbone CR, Liu X, Temm-Grove C, Sheehan SM, Hoying JB, Allen RE.** Satellite cell-mediated angiogenesis in vitro coincides with a functional hypoxia-inducible factor pathway. *Am J Physiol Cell Physiol* 296: C1321–C1328, 2009.
44. **Rosenblatt JD, Kuzon WM Jr, Plyley MJ, Pynn BR, McKee NH.** A histochemical method for the simultaneous demonstration of capillaries and fiber type in skeletal muscle. *Stain Technol* 62: 85–92, 1987.
45. **Roy RR, Hutchison DL, Pierotti DJ, Hodgson JA, Edgerton VR.** EMG patterns of rat ankle extensors and flexors during treadmill locomotion and swimming. *J Appl Physiol* 70: 2522–2529, 1991.
46. **Roy RR, Meadows ID, Baldwin KM, Edgerton VR.** Functional significance of compensatory overloaded rat fast muscle. *J Appl Physiol* 52: 473–478, 1982.
47. **Schuler M, Ali F, Metzger E, Chambon P, Metzger D.** Temporally controlled targeted somatic mutagenesis in skeletal muscles of the mouse. *Genesis* 41: 165–170, 2005.
48. **Sitnick M, Bodine SC, Rutledge JC.** Chronic high fat feeding attenuates load-induced hypertrophy in mice. *J Physiol* 587: 5753–5765, 2009.
49. **Spangenburg EE.** Changes in muscle mass with mechanical load: possible cellular mechanisms. *Appl Physiol Nutr Metab* 34: 328–335, 2009.
50. **Stauber WT, Smith CA.** Cellular responses in exertion-induced skeletal muscle injury. *Mol Cell Biochem* 179: 189–196, 1998.
51. **Tang K, Breen EC, Gerber HP, Ferrara NM, Wagner PD.** Capillary regression in vascular endothelial growth factor-deficient skeletal muscle. *Physiol Genomics* 18: 63–69, 2004.
52. **Thompson RW, McClung JM, Baltgalvis KA, Davis JM, Carson JA.** Modulation of overload-induced inflammation by aging and anabolic steroid administration. *Exp Gerontol* 41: 1136–1148, 2006.
53. **von Maltzahn J, Jones AE, Parks RJ, Rudnicki MA.** Pax7 is critical for the normal function of satellite cells in adult skeletal muscle. *Proc Natl Acad Sci USA* 110: 16474–16479, 2013.
54. **Westerkamp CM, Gordon SE.** Angiotensin-converting enzyme inhibition attenuates myonuclear addition in overloaded slow-twitch skeletal muscle. *Am J Physiol Regul Integr Comp Physiol* 289: R1223–R1231, 2005.
55. **Williams JL, Cartland D, Rudge JS, Egginton S.** VEGF trap abolishes shear stress- and overload-dependent angiogenesis in skeletal muscle. *Microcirculation* 13: 499–509, 2006.